

Journal Pre-proofs

Research paper

A new asymmetric salamo-based chemical sensor for dual channel detection of Cu^{2+} and $\text{B}_4\text{O}_7^{2-}$

Xin Xu, Ruo-Nan Bian, Shuang-Zhu Guo, Wen-Kui Dong, Yu-Jie Ding

PII: S0020-1693(20)31145-2
DOI: <https://doi.org/10.1016/j.ica.2020.119945>
Reference: ICA 119945

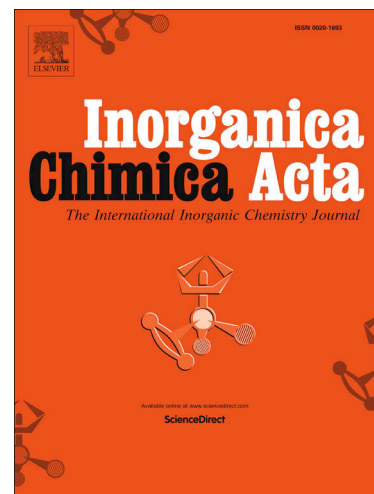
To appear in: *Inorganica Chimica Acta*

Received Date: 24 June 2020
Revised Date: 4 August 2020
Accepted Date: 5 August 2020

Please cite this article as: X. Xu, R-N. Bian, S-Z. Guo, W-K. Dong, Y-J. Ding, A new asymmetric salamo-based chemical sensor for dual channel detection of Cu^{2+} and $\text{B}_4\text{O}_7^{2-}$, *Inorganica Chimica Acta* (2020), doi: <https://doi.org/10.1016/j.ica.2020.119945>

This is a PDF file of an article that has undergone enhancements after acceptance, such as the addition of a cover page and metadata, and formatting for readability, but it is not yet the definitive version of record. This version will undergo additional copyediting, typesetting and review before it is published in its final form, but we are providing this version to give early visibility of the article. Please note that, during the production process, errors may be discovered which could affect the content, and all legal disclaimers that apply to the journal pertain.

© 2020 Published by Elsevier B.V.



A new asymmetric salamo-based chemical sensor for dual channel detection of Cu^{2+} and $\text{B}_4\text{O}_7^{2-}$

Xin Xu^a, Ruo-Nan Bian^a, Shuang-Zhu Guo^a, Wen-Kui Dong^{a,*}, Yu-Jie Ding^{b,**}

^a School of Chemical and Biological Engineering, Lanzhou Jiaotong University, Lanzhou, Gansu 730070, China

^b College of Biochemical Engineering, Anhui Polytechnic University, Wuhu 241000, China

ABSTRACT

A new type of asymmetric salamo-based colorimetric and fluorescent chemical sensor **H₂L** was synthesized and characterized. The chemical sensor **H₂L** has an efficient dual channel for Cu^{2+} and $\text{B}_4\text{O}_7^{2-}$ under the solvent conditions of DMF: $\text{H}_2\text{O} = 9: 1$ identify the effect. The oxime nitrogen and phenolic oxygen atoms in the chemical sensor **H₂L** can be used as the binding sites for Cu^{2+} . Further DFT theoretical calculations confirmed that the chemical sensor **H₂L** can combine with Cu^{2+} to form a 1: 1 complex, which in turn leads to quenching of fluorescence. Meanwhile, through ESP analysis, the N and O atoms in the chemical sensor **H₂L** have an electron donor capability, due to the introduction of $\text{B}_4\text{O}_7^{2-}$, the density of the electron cloud around the N and O atoms was changed, prompting the fluorophore of the chemical sensor **H₂L** to produce stronger fluorescence. The minimum detection limit of chemical sensor **H₂L** for Cu^{2+} is 1.99×10^{-7} M, and the minimum detection limit for $\text{B}_4\text{O}_7^{2-}$ is 7.57×10^{-7} M. In addition, the chemical sensor **H₂L** was also used to detect the Cu^{2+} content in different water samples in life.

Keywords: Asymmetric salamo-based chemical sensor, dual channel detection, PET mechanism, AIE mechanism, DFT calculation

* Corresponding author. Fax: +86 931 4938703.

** Corresponding author.

E-mail addresses: dongwk@126.com (W.-K. Dong), yujieding123@163.com (Y.-J. Ding).

1. Introduction

Copper is the oldest element used by mankind, as early 3000 BC, a bronze alloy made of copper and tin brought mankind into the bronze age [1,2]. Today, copper has been widely used in homes, industries and other places, due to its excellent ductility, electrical conductivity and corrosion resistance [3–5]. Copper can also be used as a fungicide to protect plants and crops [6,7]. In addition, copper is an indispensable important trace element in human metabolism [8,9]. Copper exists in the form of ions in the human body, it forms a complex with proteins and enzymes in human tissues, but the lack of copper will cause osteoporosis and occurrence of diseases such as heart damage, excessive intake will lead to chronic poisoning, even liver cirrhosis [10–14]. Therefore, there is a close relationship between copper and human activities, and the qualitative and quantitative detection of copper ions becomes particularly important in life [15–17].

Boron compounds are widely used in production and life [18,19]. Among them, borax and boric acid are the most important products in the boron compound series [20,21]. They are mainly used in the enamel and glass industries, which can make the enamel not easy to fall off and have gloss, and can also enhance the ultraviolet transmittance of glass, improve the transparency and heat resistance of glass [22–24]. Boron compounds have different uses in various countries, they are mainly used in the United States to manufacture glass, fiberglass, glaze and related industries [25,26], and are mainly used in detergents and glaze in Europe [27,28]. In addition, boron compounds can also be used for the manufacture of fireproof materials, boron steel and dyes, and can also be used for agricultural land disinfection to increase the boron content of the land [29–31]. Borax is highly toxic, and it is listed as a banned food additive [32,33]. If the human body consumes too much borax, it will be converted to boric acid in the role of stomach acid and absorbed by the gastrointestinal tract, but the rate of excretion is slow, and it will eventually be in the body Accumulated and poisoned [34–36]. Boron is also a necessary growth element for the human body,

animals and plants, trace amounts of boron are very beneficial to the human body, which can prevent osteoporosis and promote the metabolism of calcium in the human body [37,38]. At present, the detection of borax is mainly carried out by the titration method, which has a relatively high cost and complicated steps [39,40]. All in all, the development of fluorescent probes for qualitative and quantitative analysis becomes very necessary, but the use of salamo-based compounds for the detection of borate fluorescence is rare [41].

People are committed to designing and synthesizing high-sensitivity chemical sensors that can be quickly identified, thereby quickly and effectively detecting heavy metal ions and toxic anions [42–46]. The salamo-based compound has a good coordination environment [47–50], can form a variety of complexes with a variety of metal ions, and has the advantages of simple preparation and good selectivity [51], which makes this type of complex widely used in the field of catalysis [52,53], magnetic [54,55], luminescent [56,57], supramolecular [58,59], antioxidant activity and antibacterial materials [60,61]. In this study, a new type of chemical sensor for detecting Cu^{2+} and $\text{B}_4\text{O}_7^{2-}$ was found. It can be quantitatively identified not only by the change of fluorescence intensity, but also by the rapid qualitative detection of filter paper strips.

2. Experimental

2.1. Materials and methods

The selected reagents and solvents are analytical grade reagents of Chengdu Kelong Reagent Factory. All metal salts used in the cation test were of the molecular formula $\text{M}(\text{NO}_3)_n \cdot x\text{H}_2\text{O}$, and the sodium salt was selected for the anion test. The melting points were obtained using a micro-melting point instrument manufactured by Beijing Tyco Instrument Co., Ltd. The ^1H NMR spectra were measured on a Bruker AV 500 MHz spectrometer. Fluorescence spectrum analyses were performed on a Hitachi F-7000 FL 220-240V spectrophotometer in Tokyo, Japan. UV–Vis absorption spectra were recorded on a Shimadzu Ultraviolet-2550 spectrometer. All pH

measurements were performed using a pH-10C digital pH meter.

The fluorescence tests were performed at room temperature with a 1 cm adaptive cuvette, and a xenon lamp was used as the excitation source. Used a fluorescence spectrometer to monitor the change in fluorescence intensity ($\lambda_{\text{ex}} = 330$ nm, slit width 10 / 20 nm), and dissolved the chemical sensor **H₂L** (3.80 mg, 0.01 mmol) in 10 mL DMF: H₂O (9: 1, V / V) solution to a concentration of 1×10^{-3} mol/L, the arrangement of anionic and cationic salts was 1×10^{-2} mol/L, which was used for fluorescence testing. **All experiments were performed in Tris-HCl buffer solution with pH = 7.23.** The UV–Vis tests were also carried out at room temperature with a 1cm cuvette. Ethanol was selected as the solvent to prepare a solution with a concentration of 1×10^{-5} mol/L, anion and cation salts were also selected as a solvent with a concentration of 1×10^{-5} mol/L solution.

All quantum calculations were run using Gaussian 09, using density functional theory (DFT), using the Becke's three parameter hybrid method by using the Becke88exchange functional and LYP correlation functional (B3LYP), and selecting the 6-31G basis set for geometric optimization. The electrostatic potential (ESP) and molecular orbital analyses of the probe were done with Multiwfn 3.7, and the three-dimensional space map was drawn using VMD software.

2.2. Synthesis of the probe H₂L

The reaction procedure for the synthesis of the salamo-based chemical sensor (**H₂L**) was shown in [Scheme 1](#). 6-Methoxy-2-[O-(1-ethoxyamide)]oxime-1-phenol was synthesized according to a similar method previously reported [52,62], and an asymmetric salamo-based chemical sensor **H₂L** (6-Methoxy-2,2'-[ethylenedioxybis(nitrilomethylidyne)]phenolnaphthol) was obtained by reacting 6-methoxy-2-[O-(1-ethoxyamide)]oxime-1-phenol with 2-hydroxy-1-naphthaldehyde. Finally, a white powder was obtained in a yield of 55.3% (Based on 2-hydroxy-1-naphthaldehyde). M. p.: 113-115 °C. Anal. calcd. for C₂₁H₂₀N₂O₅: C, 66.31; H, 5.30; N, 7.36. Found: C, 61.52; H, 5.37; N, 7.28. ¹H NMR (500 MHz, CDCl₃): δ 10.82 (s, 1H), 9.80 (s, 1H), 9.18 (s, 1H), 8.28 (s, 1H), 7.97 (d, J = 8.5 Hz, 1H), 7.78 (s, 2H),

7.51 (s, 1H), 7.36 (t, $J = 7.1$ Hz, 1H), 7.20 (d, $J = 9.0$ Hz, 1H), 6.91 (dd, $J = 7.6, 1.9$ Hz, 1H), 6.85 (dd, $J = 13.9, 11.0$ Hz, 2H), 4.54 (s, 4H), 3.90 (s, 3H) (Fig. S1).

Scheme 1. Synthetic route to the chemical sensor **H₂L**.

3. Results and discussion

3.1. Solvent selection

3.1.1. Solvent effect

As a result of the solvent system have a certain influence on the fluorescence intensity of the chemical sensor, it is particularly important to choose a good solvent system for the fluorescence experiment. Eleven common organic solvents (MeOH, EtOH, DMK, THF, ACN, Py, TCM, DCM, PhH, EA and DMF) were selected to test the fluorescence intensity, and then the suitable solvents were selected for the subsequent chemical sensor **H₂L** test. The excitation wavelength of benzene with the lowest polarity was selected as the best excitation wavelength of the test, and the fluorescence spectra of the chemical sensor **H₂L** in the above solvents were tested at the same excitation wavelength. The experimental results show that the fluorescence intensity of **H₂L** in DMF solution was the strongest at 395 nm, as shown in Fig. 1. Therefore, DMF was selected as the solvent for subsequent fluorescence detection.

Fig. 1. Fluorescence intensities of **H₂L** measured under different solvents.

3.1.2. Water-containing system study

To further study the effect of mixed aqueous organic solvents on the fluorescence intensity of the chemical sensor **H₂L**, a water content test was done. In the DMF solution with different water content, the fluorescence intensity of the chemical sensor **H₂L** was shown in Fig. 2. When the water content is 10%, the fluorescence intensity of the chemical sensor **H₂L** reached the maximum value at 395 nm. As the water content increased, the fluorescence intensity decreased. When the

water content reached 70%, the chemical sensor **H₂L** appeared as a flocculent precipitate in the entire solvent system. Therefore, the mixed solvent DMF: H₂O (9: 1, V / V) was selected as the solvent used in the subsequent series of fluorescence measurements.

Fig. 2. Spectra of **H₂L** solutions (DMF) measured in different proportions of water.

3.2 Response of **H₂L** to various metal cations

3.2.1. Fluorescence response of the chemical sensor **H₂L** to cations

Based on the above experimental results, DMF: H₂O (9: 1, V / V) was selected as the fluorescence test solvent. When Cu²⁺ was added, the color of the solution changed significantly, under a normal lamp, the solution changed from a pale-yellow solution to a transparent brown solution, under a 365 nm UV lamp, the light blue color of the solution disappeared (Fig. 3).

At the excitation wavelength of 330 nm, the chemical sensor **H₂L** solution has a strong fluorescence emission peak at approximately 395 nm. After added cations to the solution of the chemical sensor **H₂L**, it was found that the fluorescence intensity of the solution was slightly enhanced, and the addition of Zn²⁺ was the most obvious. However, only after the addition of Cu²⁺, the fluorescence of the solution was completely quenched, as shown in Fig. 4a. The experimental results showed that the chemical sensor has a single recognition characteristic for Cu²⁺.

For the cause of further confirm whether other cations have an effect on the chemical sensor **H₂L** recognition of Cu²⁺, an anti-interference experiment was performed (Fig. 4b). The metal cations (Li⁺, Na⁺, K⁺, Mg²⁺, Ca²⁺, Sr²⁺, Ba²⁺, Cr³⁺, Mn²⁺, Fe³⁺, Co²⁺, Ni²⁺, Zn²⁺, Pb²⁺, Ag⁺, Cd²⁺, Al³⁺ and Hg²⁺) were added to the chemical sensor **H₂L** solution, and the fluorescence intensity was found to increase slightly. Then, Cu²⁺ was added to the above-mentioned solution containing metal ions, and the fluorescence of the solution was quenched. This indicated that other metal cations have no effect on the chemical sensor **H₂L** recognition of Cu²⁺. This result was consistent with the above identification of unity.

Fluorescence titration experiment was used to study the binding capacity of the chemical sensor **H₂L** to Cu²⁺, as shown in Fig. 4c. In 2 mL of Tris-HCl buffer solution (1×10^{-5} mol/L), added 20 μ L of the chemical sensor **H₂L** solution, and added dropwise Cu²⁺ solution of the same concentration. With the addition of Cu²⁺, fluorescence intensity of the solution gradually weakened, and until the amount of Cu²⁺ was added to 1.0 equivalent, the fluorescence of the solution was completely quenched and no longer changed, indicated that the ratio of the chemical sensor **H₂L** to Cu²⁺ was 1:1. Meanwhile, the Job working curve of the chemical sensor **H₂L** to Cu²⁺ recognition was drawn (Fig. 4d), which further confirmed **H₂L** forms a 1: 1 complex with Cu²⁺. In addition, LOD (1.99×10^{-7} M) and LOQ (6.62×10^{-7} M) were calculated (Fig. S2a) [63]. According to the Hill equation (Fig. S2b) [64,65], the binding constant *K* of **H₂L** and Cu²⁺ was estimated to be 1.36×10^9 M⁻¹. The calculation results showed that the chemical sensor **H₂L** has a high binding capacity for Cu²⁺.

Fig. 3. Comparison of the chemical sensor **H₂L** and L-Cu²⁺ solution under normal light (left), and comparison between **H₂L** and L-Cu²⁺ solution under 365 nm UV lamp (right).

Fig. 4. (a) Fluorescence spectra of **H₂L** solution (DMF: H₂O (9:1, V / V)) in the absence and presence of various metal cations (b) Fluorescence response of the L-Cu²⁺ solution to various metal ions (Li⁺, Na⁺, K⁺, Mg²⁺, Ca²⁺, Sr²⁺, Ba²⁺, Cr³⁺, Mn²⁺, Fe³⁺, Co²⁺, Ni²⁺, Zn²⁺, Pb²⁺, Ag⁺, Cd²⁺, Al³⁺ and Hg²⁺), ($\lambda_{em} = 395$ nm, $\lambda_{ex} = 330$ nm). (c) Fluorometric titration of Cu²⁺ with the chemical sensor **H₂L**. (d) Job working curve of **H₂L** identifying Cu²⁺.

3.2.2. UV-Vis response of the chemical sensor **H₂L** to cations

In order to confirm that the recognition of Cu²⁺ by the chemical sensor **H₂L** can also be determined by ultraviolet spectroscopy (Fig. 5a), various cations (Li⁺, Na⁺, K⁺, Mg²⁺, Ca²⁺, Sr²⁺, Ba²⁺, Cr³⁺, Mn²⁺, Fe³⁺, Co²⁺, Ni²⁺, Cu²⁺, Zn²⁺, Pb²⁺, Ag⁺, Cd²⁺, Al³⁺

and Hg^{2+}) were added to the solution of **H₂L** respectively, and it was found that only when Cu^{2+} was added to the chemical sensor **H₂L** solution, the UV–Vis spectra changed significantly, indicating that the chemical sensor **H₂L** could only selectively recognize Cu^{2+} . At the same time, by added Cu^{2+} to the chemical sensor **H₂L**, and then added other metal cations, the UV–Vis spectra of the solution were consistent with the UV–Vis spectrum of only added Cu^{2+} . The experimental results indicated that other cations have little interference on the recognition of Cu^{2+} by the chemical sensor **H₂L**, as shown in Fig. 5b. In addition, their binding ratio was further determined by UV–Vis titration experiments (Fig. 5c). Before the addition of Cu^{2+} , the chemical sensor **H₂L** had obvious absorption peaks at approximately 267, 302, 314, 340 and 355 nm. The absorption peak at 267 nm can be attributed to the π - π^* transition on the benzene ring of **H₂L**, and the absorption peaks at 302 and 314 nm can be attributed to the π - π^* transitions on the naphthalene ring of **H₂L**, while the absorption peaks at 340 and 355 nm can be attributed to the n- π^* transition in the **H₂L** oxime group [9,42]. When Cu^{2+} was added, the UV–Vis absorption spectra of the solution changed significantly. With the addition of Cu^{2+} , the absorption peaks at 267, 302, 314, 340 and 355 nm gradually disappeared, and new absorption peaks appeared at approximately 324 and 379 nm. These absorption peaks are mainly due to the interaction of Cu^{2+} with the oxime nitrogen portion of the chemical sensor **H₂L** and the hydroxyl oxygen on the naphthalene ring. The intramolecular hydrogen bonds of the chemical sensor **H₂L** are destroyed, increasing the coplanarity of the conjugated system. This result caused a change in the spectra of the solution. Meanwhile, when the amount of Cu^{2+} added 1.0 equivalent and continue to added, the UV–Vis spectra no longer changed, it showed that a new 1:1 complex has been formed.

Fig. 5. (a) UV–Vis spectra of the **H₂L** solution in the absence and presence of various metal cations (Li^+ , Na^+ , K^+ , Mg^{2+} , Ca^{2+} , Sr^{2+} , Ba^{2+} , Cr^{3+} , Mn^{2+} , Fe^{3+} , Co^{2+} , Ni^{2+} , Cu^{2+} , Zn^{2+} , Pb^{2+} , Ag^+ , Cd^{2+} , Al^{3+} and Hg^{2+}) (b) UV–Vis spectra of various metal cations added to L- Cu^{2+} solution. (c) UV–Vis titration of Cu^{2+} with the chemical sensor **H₂L**.

3.2.3. The mechanism of **H₂L** identifying Cu^{2+}

The DFT calculation can obtain the orbital energy of the chemical sensor and the related electron density [66,67], further indicated the recognition mechanism of the chemical sensor, and optimizing the structure of the chemical sensors **H₂L** and L-Cu^{2+} (Fig. 6).

As shown in Fig. 7, their frontier orbitals were analyzed [45,68]. In the chemical sensor **H₂L**, the HOMO and LUMO orbitals are located on the naphthalene ring with a band gap of 6.493521 eV, while in L-Cu^{2+} , the LUMO orbitals are mainly concentrated on the naphthalene ring, Cu–N and Cu–O, and the HOMO orbitals are mainly focusing on the benzene ring, Cu–N and Cu–O, the band gap is 6.118997 eV, it was indicated that electrons may be transferred from the sensor **H₂L** to the metal (LMCT), and accompanied by the PET effect. The calculated ΔE between the HOMO and LUMO of the chemical sensor **H₂L** is 6.493521 eV, and the ΔE between the HOMO and LUMO of L-Cu^{2+} is 6.118997 eV. Compared with the former, the weakened of the ΔE (0.374524 eV) of L-Cu^{2+} indicated that the coordination has occurred and a stable complex was formed (Scheme 2).

Scheme 2. Possible mechanism of Cu^{2+} recognition by chemical sensor **H₂L**.

Fig. 6. Optimized structure of **H₂L** and L-Cu^{2+} .

Fig. 7. HOMO and LUMO level orbit diagrams of **H₂L** and L-Cu^{2+} .

3.2.4. Reversible test of **H₂L** recognition of Cu^{2+}

In order to explore the cycle performance of the chemical sensor **H₂L** for Cu^{2+} recognition, a cycle performance experiment was performed (Fig. 8). Added Cu^{2+} to the **H₂L** solution, it was found that the fluorescence was turned off, and then added the complexing agent EDTA to found that the fluorescence was turned on. Continue to added Cu^{2+} and EDTA alternately, this fluorescence "on-off-on" mode will only produce a small amount of fluorescence loss during the detection process, and this

process can be repeated at least 3 times.

Finally, the previously reported literatures were compared with the binding constants and detection lines of Cu^{2+} and $\text{B}_4\text{O}_7^{2-}$ identified in this work. It can be concluded from Table 1 that the sensing performance of the chemical sensor **H₂L** in this work is superior to them [12,14,16,17,41].

Fig. 8. Reversible fluorescence experiment of **H₂L** on Cu^{2+} .

3.3 Response of **H₂L** to various anions

3.3.1. Fluorescence response of the chemical sensor **H₂L** to anions

By adding various anions (F^- , Cl^- , Br^- , I^- , HPO_4^{2-} , H_2PO_4^- , $\text{P}_2\text{O}_7^{4-}$, S^{2-} , OAc^- , CO_3^{2-} , HCO_3^- , CN^- , ClO_4^- , HS^- , NO_2^- , NO_3^- and $\text{B}_4\text{O}_7^{2-}$) to the solution of the chemical sensor **H₂L** and observing the change of the fluorescence spectra of the solution, the effect of the chemical sensor **H₂L** on the fluorescence recognition of the anion was further studied, as shown in Fig. 9a. It can be observed from the fluorescence spectra that the chemical sensor **H₂L** solution has a strong fluorescence emission peak at approximately 395 nm. When $\text{B}_4\text{O}_7^{2-}$ was added to the above solution, the fluorescence intensity of the solution disappeared at 395 nm, and a new strong fluorescence emission peak appeared at approximately 471 nm. When other anions were added to the chemical sensor **H₂L** solution, the fluorescence intensities of the solution showed almost no significant change at 395 nm. The experimental results showed that the chemical sensor **H₂L** can effectively detect $\text{B}_4\text{O}_7^{2-}$ in many common anions. In addition, the fluorescence of the solution changed under normal lamp and 365 nm UV-Vis lamp can be observed in the inset.

The anti-interference test further confirmed whether other anions had any effect on the recognition of $\text{B}_4\text{O}_7^{2-}$. As shown in Fig. 9b, the fluorescence intensity at the emission wavelength of 471 nm was selected. The other anions were added to the solution of the chemical sensor **H₂L**, and the solution had almost no fluorescence at 471 nm. When $\text{B}_4\text{O}_7^{2-}$ was added to the above solution containing anions, the solution showed strong fluorescence at 471 nm. The experimental results showed that the

chemical sensor **H₂L** only selectively recognizes the anion $\text{B}_4\text{O}_7^{2-}$ and other anions had no interference.

At the same time, $\text{B}_4\text{O}_7^{2-}$ solution was slowly added to the chemical sensor **H₂L** solution in order to study the binding capacity of the chemical sensor **H₂L** to $\text{B}_4\text{O}_7^{2-}$. When 4.0 equivalents of $\text{B}_4\text{O}_7^{2-}$ solution were added to the above solution, the fluorescence intensity no longer changed, as shown in Fig. 9c. The experimental results showed that the chemical sensor **H₂L** and $\text{B}_4\text{O}_7^{2-}$ were combined in the formation of 1: 4. In addition, LOD (7.57×10^{-7} M) and LOQ (2.52×10^{-6} M) were calculated (Fig. S3a). Through the Hill equation (Fig. S3b), it can be speculated that the binding constant K of **H₂L** and $\text{B}_4\text{O}_7^{2-}$ is $2.17 \times 10^9 \text{ M}^{-1}$, indicating that the binding ability of **H₂L** and $\text{B}_4\text{O}_7^{2-}$ was very high.

Fig. 9. (a) Fluorescence emission spectra of **H₂L** solution in the presence of different anions (F^- , Cl^- , Br^- , I^- , HPO_4^{2-} , H_2PO_4^- , $\text{P}_2\text{O}_7^{4-}$, S^{2-} , OAc^- , CO_3^{2-} , HCO_3^- , CN^- , ClO_4^- , HS^- , NO_2^- , NO_3^- and $\text{B}_4\text{O}_7^{2-}$). (b) Fluorescence response of **L-B₄O₇²⁻** solution to other anions ($\lambda_{\text{em}} = 395 \text{ nm}$, $\lambda_{\text{ex}} = 330 \text{ nm}$). (c) Titration of $\text{B}_4\text{O}_7^{2-}$ into **H₂L** solution.

3.3.2. UV-Vis response of the chemical sensor **H₂L** to anions

In order to confirm the recognition of $\text{B}_4\text{O}_7^{2-}$ by the chemical sensor **H₂L**, it can also be determined by UV-Vis absorption spectra (Fig. 10a). Various anions were added to the chemical sensor **H₂L** solution, only after adding $\text{B}_4\text{O}_7^{2-}$, the UV-Vis absorption spectrum of the solution changed significantly. When other anions were added, the UV-Vis absorption spectra of the solution did not change significantly. At the same time, through anti-interference experiments to further verify that other anions have no significant effect on the chemical sensor **H₂L** recognition of $\text{B}_4\text{O}_7^{2-}$, as shown in Fig. 10b. In addition, the ultraviolet absorption spectrum of the chemical sensor **H₂L** recognizing $\text{B}_4\text{O}_7^{2-}$ was observed through an ultraviolet titration experiment (Fig. 10c). With the increase of the amount of $\text{B}_4\text{O}_7^{2-}$, the absorption peak of the solution shifted from 267 nm to 262 nm compared with the chemical sensor

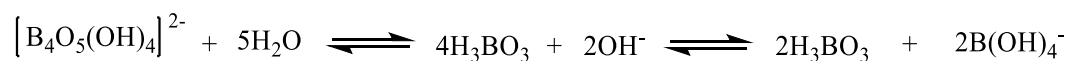
H₂L, and the ultraviolet absorption peaks at approximately 302, 314 and 340 nm were slightly enhanced, but a new UV–Vis characteristic absorption peak appeared at 384 nm.

Fig. 10. (a) UV–Vis spectra of the chemical sensor **H₂L** in the presence of various cations. (b) UV–Vis absorption competitive response of **H₂L** solutions to various metal ions. (c) UV–Vis absorption spectra of **H₂L** after addition of $B_4O_7^{2-}$ (0–4.0 equiv.).

3.3.3. The mechanism of **H₂L** identifying $B_4O_7^{2-}$

For the cause of better the sensing mechanism, the electrostatic potential of the chemical sensor **H₂L** was analyzed [67]. The electrostatic potential (ESP) was of great significance for investigating electrostatic interactions between molecules, predicting molecular properties, and predicting reaction sites, as shown in Fig. 11, different electrostatic potentials on the molecular surface were represented by different colors, where blue represents negative electrostatic potential and red represents positive electrostatic potential. The distribution of the electrostatic potential of the molecule was mainly the positive potential, which can be attributed to the hydrogen atoms at the edge of the benzene ring and naphthalene ring of the chemical sensor **H₂L** participated in the formation of the C–H bond. The negative electrostatic potential around the benzene and naphthalene ring in the molecule was the π electronic feature, while the N and O atoms negative electrostatic potential distribution because N and O have strong electron withdrawing ability, and can act as electron acceptors by forming other new complexes.

Borate could be hydrolyzed to boric acid was the main reason led to fluorescence quenched:



Since the N and O atoms in the chemical sensor **H₂L** can be used as electron donor, the special structure of boric acid easily enters the **H₂L** conjugate system, boric acid molecules can spontaneously form intermolecular hydrogen bonds, and can extend to form a two-dimensional periodic structure, which also makes the boric acid molecules in a state of aggregation in solution, leading to the occurrence of fluorescence aggregation-induced emission (AIE) effect. Therefore, the fluorescence of the chemical sensor **H₂L** was significantly enhanced.

Fig. 11. Electrostatic potential (ESP) diagram for **H₂L**.

3.4 Effect of pH on the chemical sensor **H₂L**

In order to investigate whether the chemical sensor **H₂L** can recognize Cu^{2+} and $\text{B}_4\text{O}_7^{2-}$ in a physiological environment, a pH response study was conducted (Fig. 12) [44]. When the pH value was 1~3, the chemical sensor **H₂L** may lose its activity in a strong acid system, resulting in a decrease in the fluorescence intensity of the solution, between pH 4~12, the fluorescence intensity of **H₂L** was stable. When Cu^{2+} was added to the solution of the chemical sensor **H₂L**, it was found that the fluorescence intensity of the solution was significantly reduced in the pH range of 4~10 at 395 nm and tended to be stable, indicating that the recognition of Cu^{2+} by **H₂L** can be applied in the range of pH 4~10. When $\text{B}_4\text{O}_7^{2-}$ was added to the chemical sensor **H₂L**, in the pH range of 1~3, the solution has almost no fluorescence at 471 nm, and in the pH range of 4~8, the solution has the strongest fluorescence and almost no obvious fluctuation. The above experimental results showed that the chemical sensor **H₂L** can recognize Cu^{2+} and $\text{B}_4\text{O}_7^{2-}$ in the pH range applicable to the physiological environment.

Fig. 12. Fluorescence intensity at different pH.

3.5 Time response of the chemical sensor **H₂L**

The rapid recognition of Cu^{2+} and $\text{B}_4\text{O}_7^{2-}$ by the chemical sensor **H₂L** was further studied, and the time response experiment was carried out (Fig. 13) [43]. When Cu^{2+} was added to the chemical sensor **H₂L**, the fluorescence of the solution immediately quenched at 395 nm within 10 seconds. According to the same method as above, when $\text{B}_4\text{O}_7^{2-}$ was added to the chemical sensor **H₂L**, the fluorescence of the solution immediately increased significantly at 471 nm within 10 seconds, and the fluorescence intensity no longer changed within 1 minute. The experimental results showed that the chemical sensor **H₂L** can quickly identify Cu^{2+} and $\text{B}_4\text{O}_7^{2-}$.

Fig. 13. Fluorescence intensity at different time.

3.6 Practical application of the chemical sensor **H₂L**

In order to evaluate the practicality of the chemical sensor **H₂L** in life, it can be used to detect the Cu^{2+} content in different water samples [43,48]. Added 28 μM Cu^{2+} to different water samples, and analyzed the test samples by standard addition methods used fluorescence spectroscopy. As shown in Fig. 14 and Table 2, the Cu^{2+} content of tap water, river water and rain water was measured to be 2.75, 3.83 and 5.21 μM , respectively. Repeat the test 3 times in the same way, and the relative standard deviation (RSD) is within 5%. The experimental results showed that the chemical sensor **H₂L** can be used for quantitative detection of Cu^{2+} in different water samples.

Fig. 14. The chemical sensor **H₂L** detects the fluorescence intensities of Cu^{2+} in different water samples.

Although the chemical sensor **H₂L** has excellent performance in detecting Cu^{2+} and $\text{B}_4\text{O}_7^{2-}$, it still has certain challenges as a cost-effective chemical sensor [46]. Therefore, it is very important to use a test strip for rapid testing. Immerse the filter paper treated with dilute hydrochloric acid in the **H₂L** solution of DMF: H_2O (9:1, V / V) with a concentration of 1×10^{-3} mol/L. After the load is uniform, place the test

paper in a vacuum drying oven dry at low temperature. The test strip containing **H₂L** showed light blue fluorescence. When Cu^{2+} interacted, the fluorescence was turned off, while other metal cations did not change under ultraviolet light (Fig. 15a). When $\text{B}_4\text{O}_7^{2-}$ was added, the fluorescence was significantly enhanced, showing a clear blue fluorescence under the UV lamp, and other anions did not have this change (Fig. 15b). The experimental results showed that the test strip can be used for qualitative analyses of Cu^{2+} and $\text{B}_4\text{O}_7^{2-}$ (Fig. 15c).

Fig. 15. Test strip color change (a) with various metal ions (b) anions and (c) Cu^{2+} and $\text{B}_4\text{O}_7^{2-}$ response. (Under 365 nm UV lamp).

4. Conclusions

In this work, a new type of salamo-based chemical sensor **H₂L** was synthesized, which can be used for qualitative and quantitative analyses of Cu^{2+} and $\text{B}_4\text{O}_7^{2-}$. According to the calculation of the frontier orbit by DFT, the chemical sensor **H₂L** and Cu^{2+} formed a stable 1:1 complex, which caused the fluorescence to turn off. The identification of $\text{B}_4\text{O}_7^{2-}$ was mainly due to the formation of H_3BO_3 by hydrolysis. H_3BO_3 has a unique structure, which will further affect the electronic density of the chemical sensor **H₂L**. Through the analysis of the electrostatic potential (ESP) of **H₂L**, it can be clearly seen that the N and O atoms can act as electron donor, and aggregation-induced emission (AIE), which in turn leads to a sharp increase in fluorescence. Finally, the chemical sensor **H₂L** can quantitatively test the Cu^{2+} content in different water samples in real life, and obtain a test strip for rapid testing of Cu^{2+} and $\text{B}_4\text{O}_7^{2-}$.

Declarations of interest:

The authors declare no conflict of interest.

Acknowledgements

This work was supported by the National Natural Science Foundation of China (21761018) and the Program for Excellent Team of Scientific Research in Lanzhou Jiaotong University (201706), both of which are gratefully acknowledged.

Journal Pre-proofs

References

- [1] A. Sumiyoshi, Y. Chiba, R. Matsuoka, T. Noda, T. Nabeshima, *Dalton Trans.* 48 (2019) 13169.
- [2] S. Akine, Z. Varadi, T. Nabeshima, *Eur. J. Inorg. Chem.* 2013 (2013) 5987.
- [3] H.R. Mu, M. Yu, L. Wang, Y. Zhang, Y.J. Ding, *Phosphorus Sulfur Silicon Relat. Elem.* 195 (2020) 730.
- [4] Y.X. Sun, Y.Q. Pan, X. Xu, Y. Zhang, *Crystals* 9 (2019) 607.
- [5] S.Z. Zhang, J. Chang, H.J. Zhang, Y.X. Sun, Y. Wu, Y. B. Wang, *Chin. J. Inorg. Chem.* 36 (2020) 503.
- [6] T. Nakamura, S. Tsukuda, T. Nabeshima, *J. Am. Chem. Soc.* 141 (2019) 6462.
- [7] G. Kumar, D. Kumar, S. Devi, R. Johari, C.P. Singh, *Eur. J. Med. Chem.* 45 (2010) 3056.
- [8] Q.P. Kang, X.Y. Li, L. Wang, Y. Zhang, W.K. Dong, *Appl. Organomet. Chem.* 33 (2019) e5013.
- [9] Y.Q. Pan, X. Xu, Y. Zhang, Y. Zhang, W.K. Dong, *Spectrochim. Acta A* 229 (2020) 117927.
- [10] M.J. Timm, L. Leung, K. Anggara, T. Lim, Z. Hu, S. Latini, A. Rubio, J.C. Polanyi, *J. Am. Chem. Soc.* 142 (2020) 9453.
- [11] P.K. Muwal, A. Nayal, M.K. Jaiswal, P.S. Pandey, *Tetrahedron Lett.* 59 (2018) 29.
- [12] M. Tian, H. He, B.B. Wang, X. Wang, Y. Liu, F.L. Jiang, *Dyes Pigm.* 165 (2019) 383.
- [13] A. Kumar, S. Kumar, P.S. Chae, *Dyes Pigm.* 181 (2020) 108522.
- [14] M. Sahu, A. Kumar Manna, K. Rout, J. Mondal, G.K. Patra, *Inorg. Chim. Acta* 508 (2020) 119633.
- [15] Z.Y. Gündüz, C. Gündüz, C. Özpınar, O.A. Urucu, *Spectrochim. Acta A* 136 (2015) 1679.
- [16] A.K. Manna, K. Rout, S. Chowdhury, G.K. Patra, *Photochem. Photobio. Sci.* 18 (2019) 1512.
- [17] H. Fang, P.C. Huang, F.Y. Wu, *Spectrochim. Acta A* 204 (2018) 568.
- [18] K. Wang, T. Yin, H. Zhou, X. Liu, J. Deng, S. Li, C. Lu, X. Chen, *J. Eur. Ceram. Soc.* 40 (2020) 381.
- [19] L. Li, F. Wang, Q. Liao, Y. Wang, H. Zhu, Y. Zhu, *J. Nucl. Mater.* 528 (2020) 151854.
- [20] L. Yan, C. Du, M. Riaz, C. Jiang, *Environ. Pollut.* 255 (2019) 113254.
- [21] M. Chen, O. Dollar, K. Shafer-Peltier, S. Randtke, S. Waseem, E. Peltier, *Water Res.* 170 (2020) 115362.

- [22] C.Y. Pan, L.J. Zhong, F.H. Zhao, Y.Z. Luo, D.G. Li, *Inorg. Chem.* 54 (2015) 403.
- [23] C. Wu, L. Li, J. Song, G. Yang, M.G. Humphrey, C. Zhang, *Inorg. Chem.* 56 (2017) 1340.
- [24] J. Li, Z. Liu, Y. Wang, R. Wang, *J. Alloys Compd.* 834 (2020) 155150.
- [25] F. Spadaro, A. Rossi, S.N. Ramakrishna, E. Laine, P. Woodward, N.D. Spencer, *Langmuir*. 34 (2018) 2219.
- [26] K.G. Yves, T. Chen, J.T. Aladejana, Z. Wu, Y. Xie, *ACS Omega* 5 (2020) 8784.
- [27] B. Cicek, E. Karadagli, F. Duman, *Ceram. Int.* 44 (2018) 14264.
- [28] T.S. Ortner, K. Wurst, M. Seibald, B. Joachim, H. Huppertz, *Eur. J. Inorg. Chem.* 2016 (2016) 3292.
- [29] A. Vera, J.L. Moreno, C. Garcia, D. Morais, F. Bastida, *Sci. Total Environ.* 685 (2019) 564.
- [30] R.T. Ioto, C.A. Loto, M. Akinyele, *Alex. Eng. J.* 59 (2020) 933.
- [31] M. Liu, Q. Guo, L. Luo, T. He, *J. Volcanol. Geotherm. Res.* 397 (2020) 106887.
- [32] H.A. Saudi, W.M. Abd-Allah, K.S. Shaaban, *J. Mater. Sci. Mater. Electron.* 31 (2020) 6963.
- [33] L.A.L. Dias, W.A. Alves, *J. Mol. Liq.* 289 (2019) 111152.
- [34] F. Risplendi, F. Raffone, L.C. Lin, J.C. Grossman, G. Cicero, *J. Phys. Chem. C* 124 (2020) 1438.
- [35] S. Tursunbadalov, L. Soliev, *J. Chem. Eng. Data* 63 (2018) 598.
- [36] G. Kuz'micheva, R. Svetogorov, I. Kaurova, *J. Solid State Chem.* 288 (2020) 121393.
- [37] X. Zhou, J. Huang, G. Cai, H. Zhou, Y. Huang, X. Su, *Dalton Trans.* 49 (2020) 3284.
- [38] X. Cui, J. Wang, M. Wen, X. Dai, K. Miao, K. Wang, K. Zhang, *Ceram. Int.* 46 (2020) 9854.
- [39] X. Ding, Y. Gu, Q. Li, B.h. Kim, Q. Wang, J. Huang, *Ceram. Int.* 46 (2020) 13225.
- [40] H. Morito, S. Shibano, T. Yamada, T. Ikeda, M. Terauchi, R.V. Belosludov, H. Yamane, *Solid State Sci.* 102 (2020) 106166.
- [41] L.M. Pu, X.Y. Li, J. Hao, Y.X. Sun, Y. Zhang, H.T. Long, W.K. Dong, *Sci. Rep.* 8 (2018) 14058.
- [42] L. Wang, Z.L. Wei, Z.Z. Chen, C. Liu, W.K. Dong, Y.J. Ding, *Microchem. J.* 155 (2020) 104801.
- [43] L. Wang, Y.Q. Pan, J.F. Wang, Y. Zhang, Y.J. Ding, *J. Photochem. Photobio. A* 400 (2020) 112719.
- [44] W.K. Dong, S.F. Akogun, Y. Zhang, Y.X. Sun, X.Y. Dong, *Sens. Actuators B* 238 (2017) 723.

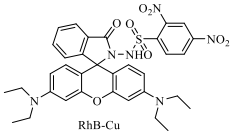
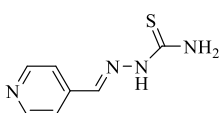
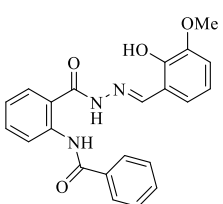
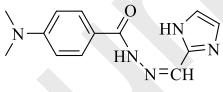
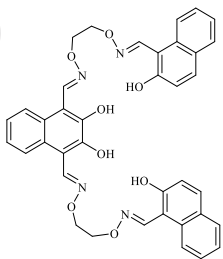
- [45] F. dos Santos Carlos, L.A. da Silva, C. Zanlorenzi, F. Souza Nunes, *Inorg. Chim. Acta* 508 (2020) 119634.
- [46] S. Saravana Kumar, R. Selva Kumar, S.K. Ashok Kumar, *Inorg. Chim. Acta* 502 (2020) 119348.
- [47] J. Chang, S.Z. Zhang, Y. Wu, H.J. Zhang, Y.X. Sun, *Transit. Met. Chem.* 45 (2020) 279.
- [48] Z.L. Wei, L. Wang, J.F. Wang, W.T. Guo, Y. Zhang, W.K. Dong, *Spectrochim. Acta A* 228 (2020) 117775.
- [49] M. Yu, Y. Zhang, Y.Q. Pan, L. Wang, *Inorg. Chim. Acta* 509 (2020) 119701.
- [50] Y.Q. Pan, Y. Zhang, M. Yu, Y. Zhang, L. Wang, *Appl. Organomet. Chem.* 34 (2020) e5441.
- [51] L.W. Zhang, Y. Zhang, Y.F. Cui, M. Yu, W.K. Dong, *Inorg. Chim. Acta* 506 (2020) 119534.
- [52] X.X. An, Z.Z. Chen, H.R. Mu, L. Zhao, *Inorg. Chim. Acta* 511 (2020) 119823.
- [53] C. Liu, X.X. An, Y.F. Cui, K.F. Xie, W.K. Dong, *Appl. Organomet. Chem.* 34 (2019) e5272.
- [54] X.Y. Li, Q.P. Kang, C. Liu, Y. Zhang, W.K. Dong, *New J. Chem.* 43 (2019) 4605.
- [55] L.Z. Liu, M. Yu, X.Y. Li, Q.P. Kang, W.K. Dong, *Chin. J. Inorg. Chem.* 35 (2019) 1283.
- [56] H.R. Mu, X.X. An, C. Liu, Y. Zhang, W.K. Dong, *J. Struct. Chem.* 61 (2020) 1218.
- [57] Y. Zhang, L.Z. Liu, Y.D. Peng, N. Li, W.K. Dong, *Transit. Met. Chem.* 44 (2019) 627.
- [58] Q.P. Kang, X.Y. Li, Z.L. Wei, Y. Zhang, W.K. Dong, *Polyhedron* 165 (2019) 38.
- [59] Q. Zhao, X.X. An, L.Z. Liu, W.K. Dong, *Inorg. Chim. Acta* 490 (2019) 6.
- [60] M. Yu, H.R. Mu, L.Z. Liu, N. Li, Y. Bai, X.Y. Dong, *Chin. J. Inorg. Chem.* 35 (2019) 1109.
- [61] Y. Zhang, M. Yu, Y. Q. Pan, Y. Zhang, L. Xu, X. Y. Dong, *Appl. Organomet. Chem.* 34 (2020) e5442.
- [62] R.Y. Li, X.X. An, J.L. Wu, Y.P. Zhang, W.K. Dong, *Crystals* 9 (2019) 408.
- [63] L.Z. Liu, L. Wang, M. Yu, Q. Zhao, Y. Zhang, Y.X. Sun, W.K. Dong, *Spectrochim. Acta A* 222 (2019) 117209.
- [64] L. Wang, Z.L. Wei, C. Liu, W.K. Dong, J.X. Ru, *Spectrochim. Acta A* 239 (2020) 118496.
- [65] C. Liu, Z.L. Wei, H.R. Mu, W.K. Dong, Y.J. Ding, *J. Photochem. Photobio. A* 397 (2020) 112569.
- [66] S. Akine, M. Miyashita, T. Nabeshima, *Chem. Eur. J.* 25 (2019) 1432.
- [67] T. Hojo, T. Nakamura, R. Matsuoka, T. Nabeshima, *Heteroatom Chem.* 29 (2018) e21470.
- [68] J.C. Deems, J.H. Reibenspies, H.S. Lee, R.D. Hancock, *Inorg. Chim. Acta* 499 (2020)

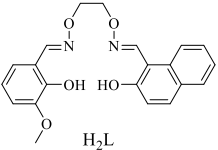
119181.

Journal Pre-proofs

Table 1

Comparison of binding constants and detection lines between chemosensors.

No.	sensor	Binding constant (M ⁻¹)	Detection limit (M)	Identification substance	pH range	Reference
1		6.42×10^4	4.7×10^{-6}	Cu ²⁺	4~8	[12]
2		2.4×10^2	1.7×10^{-6}	Cu ²⁺	4~12	[14]
3		1.39×10^4	1.89×10^{-6}	Cu ²⁺	3~13	[16]
4		4.3×10^7	1.2×10^{-7}	Cu ²⁺	None	[17]
5		4.72×10^3	8.61×10^{-7}	B ₄ O ₇ ²⁻	1~7	[41]

6	 H ₂ L	1.36×10^9	1.99×10^{-7}	Cu ²⁺	4~10	This work
		2.17×10^9	7.57×10^{-7}	B ₄ O ₇ ²⁻	4~8	This work

Journal Pre-proofs

Table 2Probe **H₂L** to detect different water samples.

Sample	Added Cu ²⁺ (μ M)	Found (μ M)	Recovery (%)	R.S.D. (n = 3) (%)
Tap water	28.0	30.75	109.8	1.2
river water	28.0	31.83	113.7	0.97
rain water	28.0	33.21	118.6	1.16

LEGENDS**Scheme 1.** Synthetic route to the chemical sensor **H₂L**.**Scheme 2.** Possible mechanism of Cu²⁺ recognition by probe **H₂L**.**Fig. 1.** Fluorescence intensities of **H₂L** measured under different solvents.**Fig. 2.** Spectra of **H₂L** solutions (DMF) measured in different proportions of water.**Fig. 3.** Comparison of the chemical sensor **H₂L** and L-Cu²⁺ solution under normal light (left), and comparison between **H₂L** and L-Cu²⁺ solution under 365nm UV lamp (right).**Fig. 4.** (a) Fluorescence spectra of **H₂L** solution (DMF: H₂O (9:1, V / V)) in the absence and presence of various metal cations (b) Fluorescence response of the L-Cu²⁺ solution to various metal ions (Li⁺, Na⁺, K⁺, Mg²⁺, Ca²⁺, Sr²⁺, Ba²⁺, Cr³⁺, Mn²⁺, Fe³⁺, Co²⁺, Ni²⁺, Zn²⁺, Pb²⁺, Ag⁺, Cd²⁺, Al³⁺ and Hg²⁺), ($\lambda_{em} = 395$ nm, $\lambda_{ex} = 330$ nm). (c) Fluorometric titration of Cu²⁺ with the chemical sensor **H₂L**. (d) Job working curve of **H₂L** identifying Cu²⁺.**Fig. 5.** (a) UV–Vis spectra of the **H₂L** solution in the absence and presence of various metal cations (Li⁺, Na⁺, K⁺, Mg²⁺, Ca²⁺, Sr²⁺, Ba²⁺, Cr³⁺, Mn²⁺, Fe³⁺, Co²⁺, Ni²⁺, Cu²⁺,

Zn²⁺, Pb²⁺, Ag⁺, Cd²⁺, Al³⁺ and Hg²⁺) (b) UV–Vis spectra of various metal cations added to L-Cu²⁺ solution. (c) UV–Vis titration of Cu²⁺ with the chemical sensor **H₂L**.

Fig. 6. Optimized structure of **H₂L** and L-Cu²⁺.

Fig. 7. HOMO and LUMO level orbit diagrams of **H₂L** and L-Cu²⁺.

Fig. 8. Reversible fluorescence experiment of **H₂L** on Cu²⁺.

Fig. 9. (a) Fluorescence emission spectra of **H₂L** solution in the presence of different anions (F⁻, Cl⁻, Br⁻, I⁻, HPO₄²⁻, H₂PO₄⁻, P₂O₇⁴⁻, S²⁻, OAc⁻, CO₃²⁻, HCO₃⁻, CN⁻, ClO₄⁻, HS⁻, NO₂⁻, NO₃⁻ and B₄O₇²⁻). (b) Fluorescence response of **L-B₄O₇²⁻** solution to other anions ($\lambda_{em} = 471 \text{ nm}$, $\lambda_{ex} = 330 \text{ nm}$). (c) Titration of B₄O₇²⁻ into **H₂L** solution.

Fig. 10. (a) UV–Vis spectra of the chemical sensor **H₂L** in the presence of various cations. (b) UV–Vis absorption competitive response of **H₂L** solutions to various metal ions. (c) UV–Vis absorption spectra of **H₂L** after addition of B₄O₇²⁻ (0–4.0 equiv.).

Fig. 11. Electrostatic potential (ESP) diagram for **H₂L**.

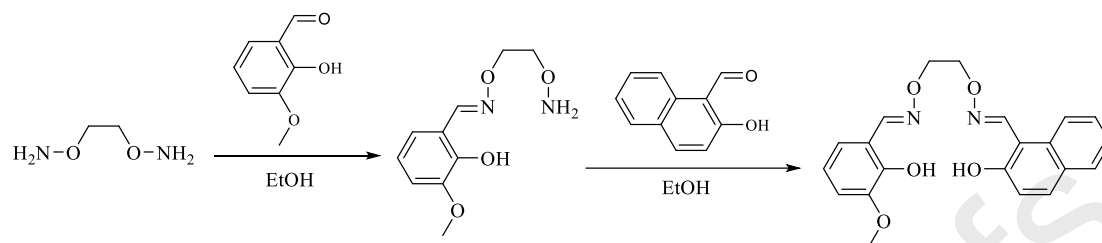
Fig. 12. Fluorescence intensity at different pH.

Fig. 13. Fluorescence intensity at different time.

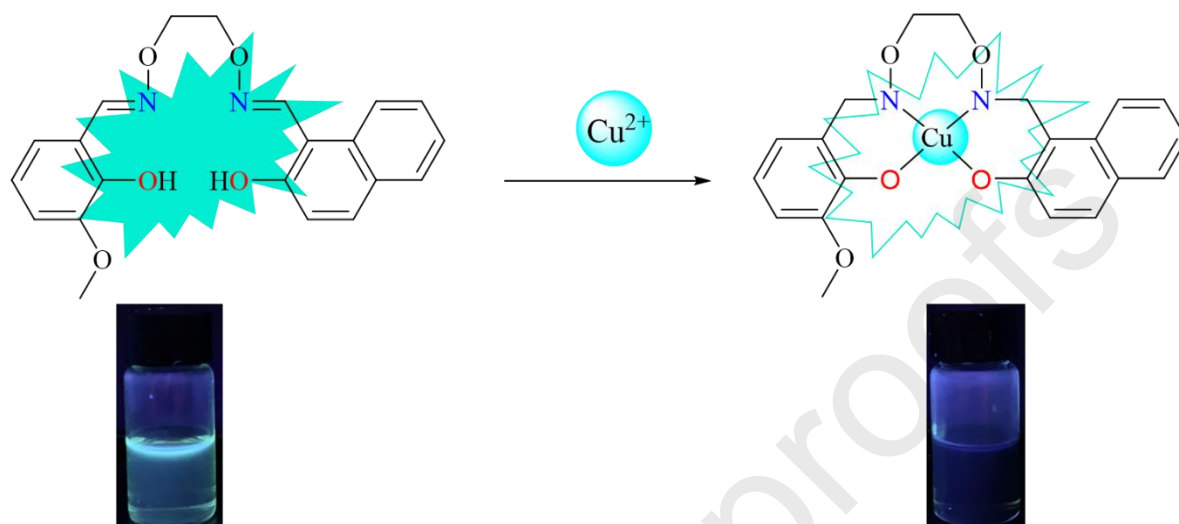
Fig. 14. The chemical sensor **H₂L** detects the fluorescence intensities of Cu²⁺ in different water samples.

Fig. 15. Test strip color change (a) with various metal ions (b) anions and (c) Cu^{2+} and $\text{B}_4\text{O}_7^{2-}$ response. (Under 365 nm UV lamp).

Journal Pre-proofs



Scheme 1.



Scheme 2.

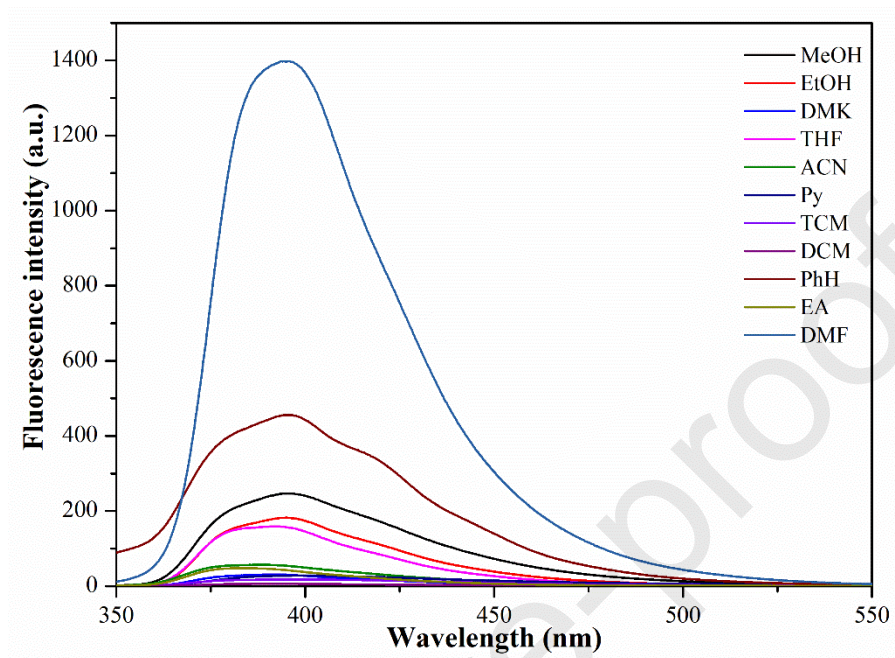


Fig. 1

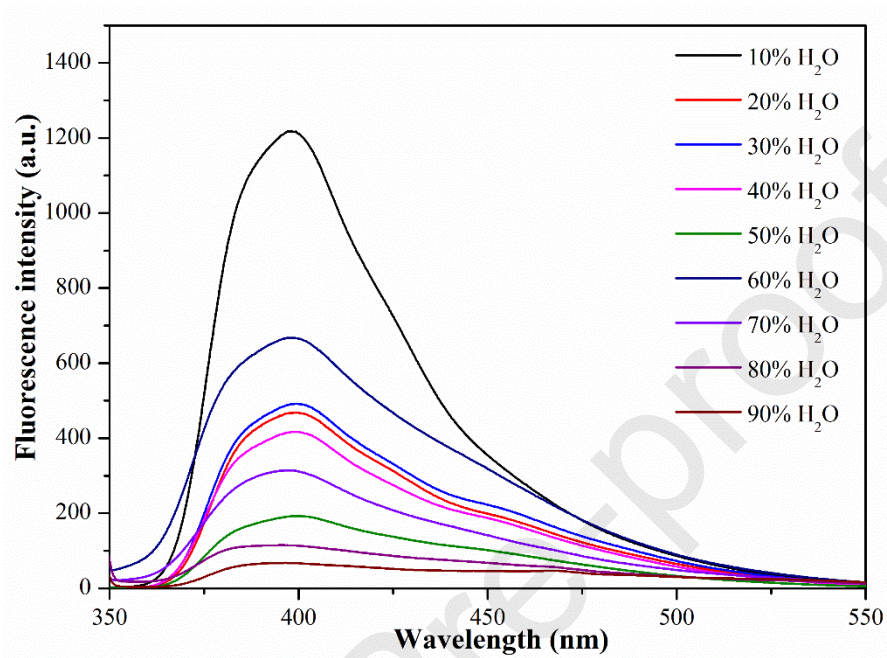
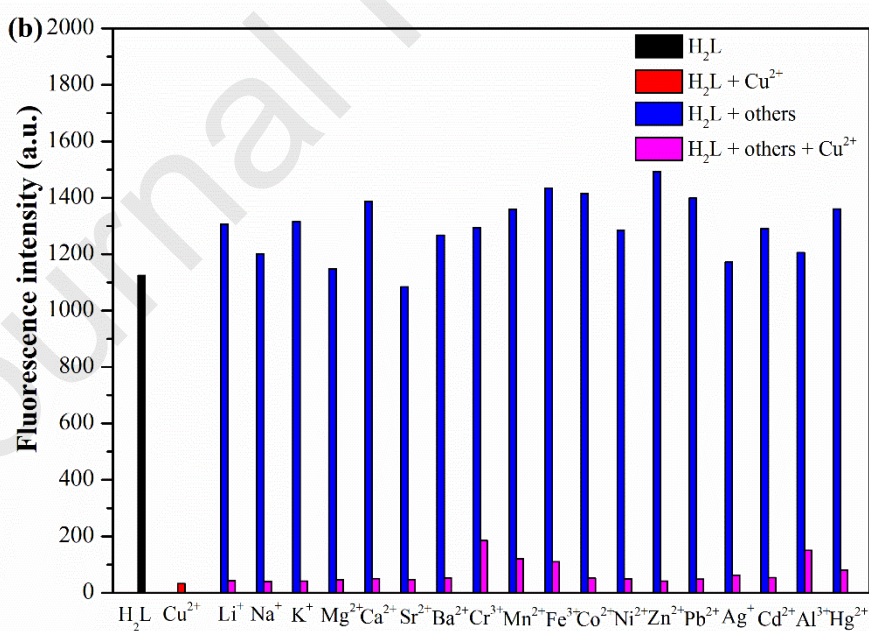
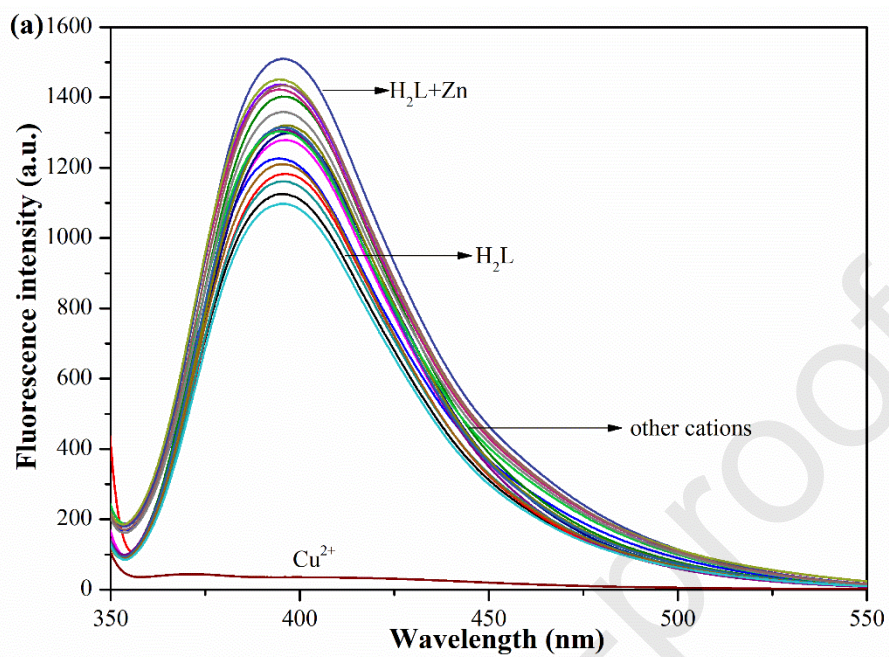


Fig. 2



Fig. 3



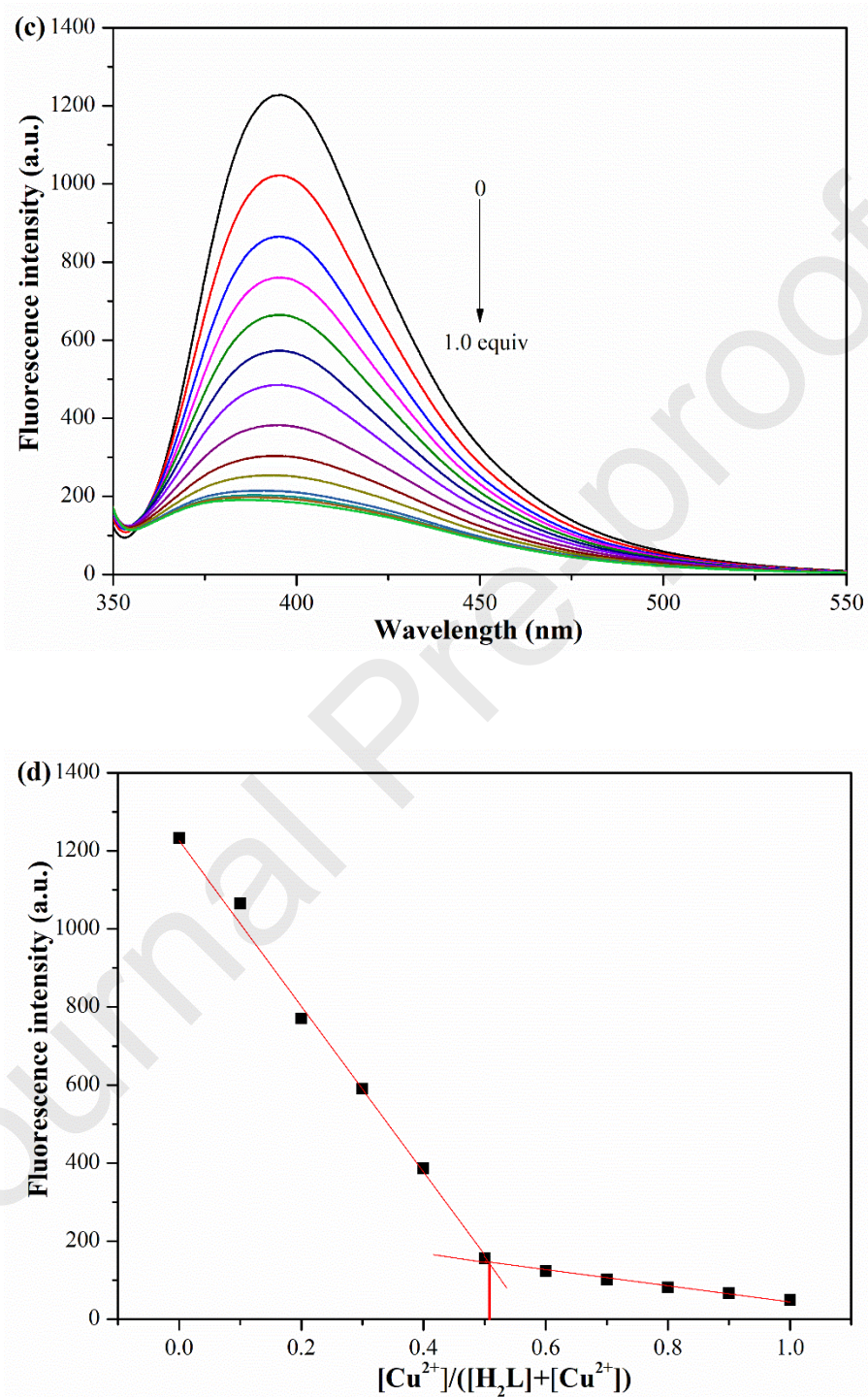
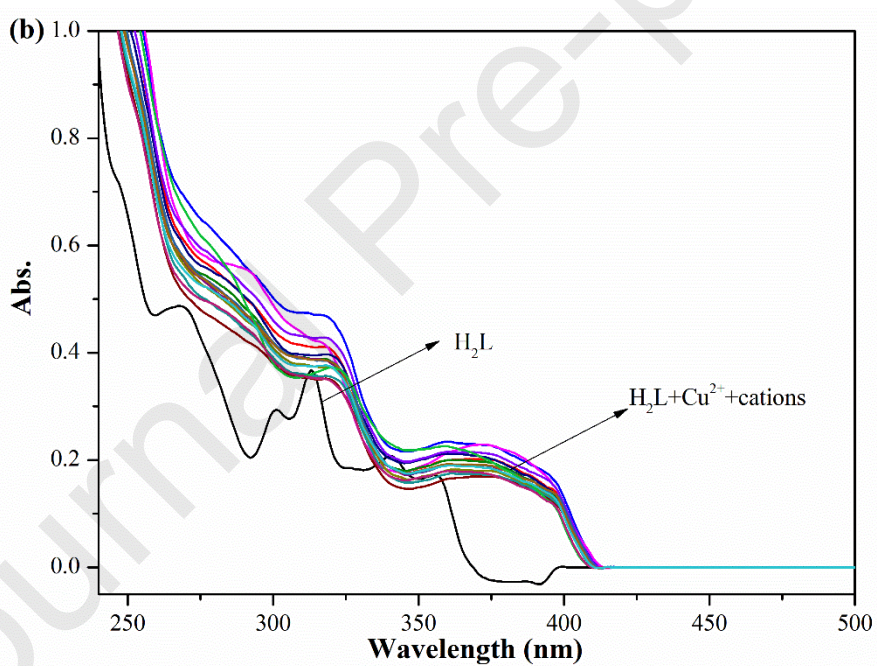
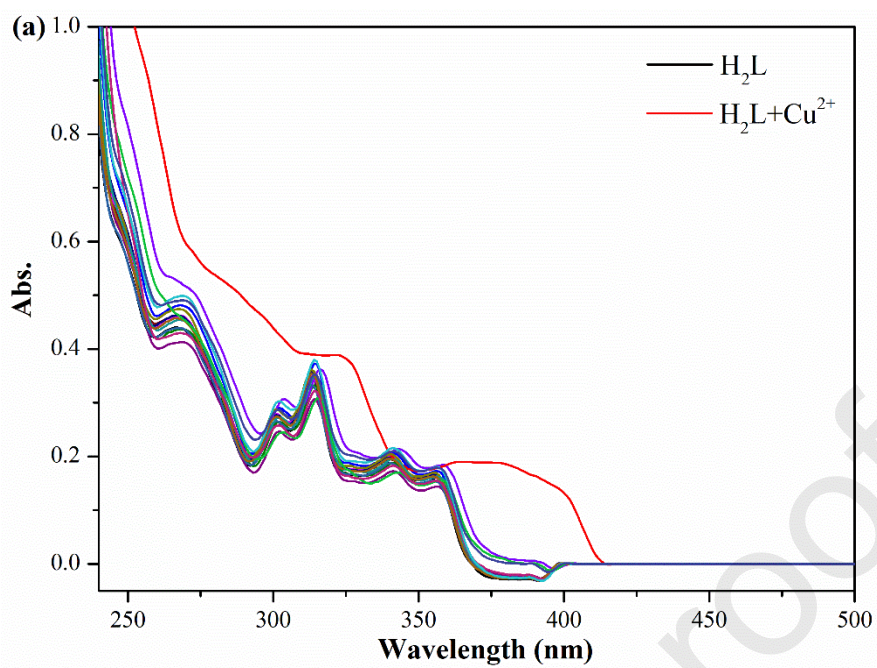


Fig. 4



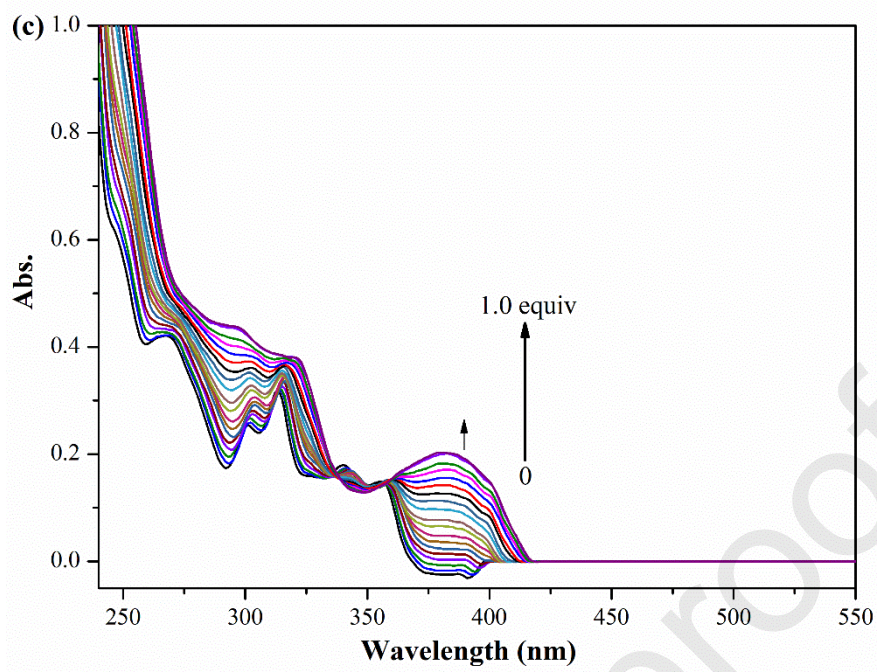


Fig. 5

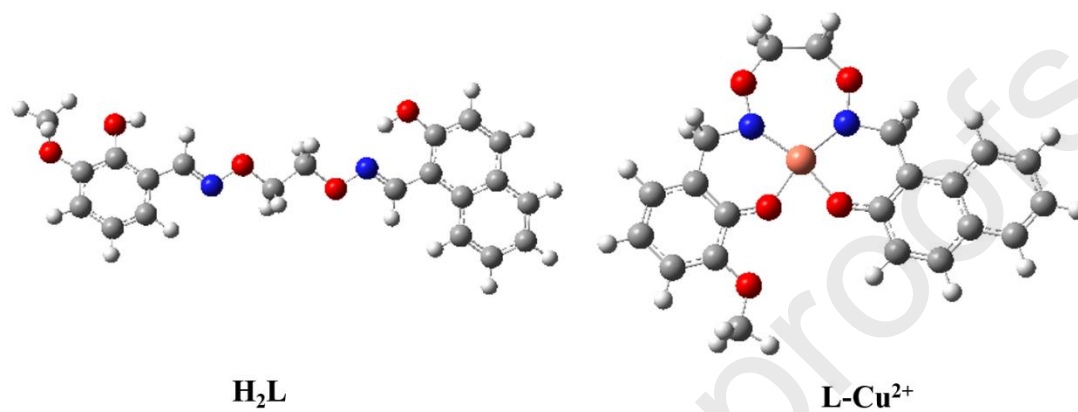


Fig. 6

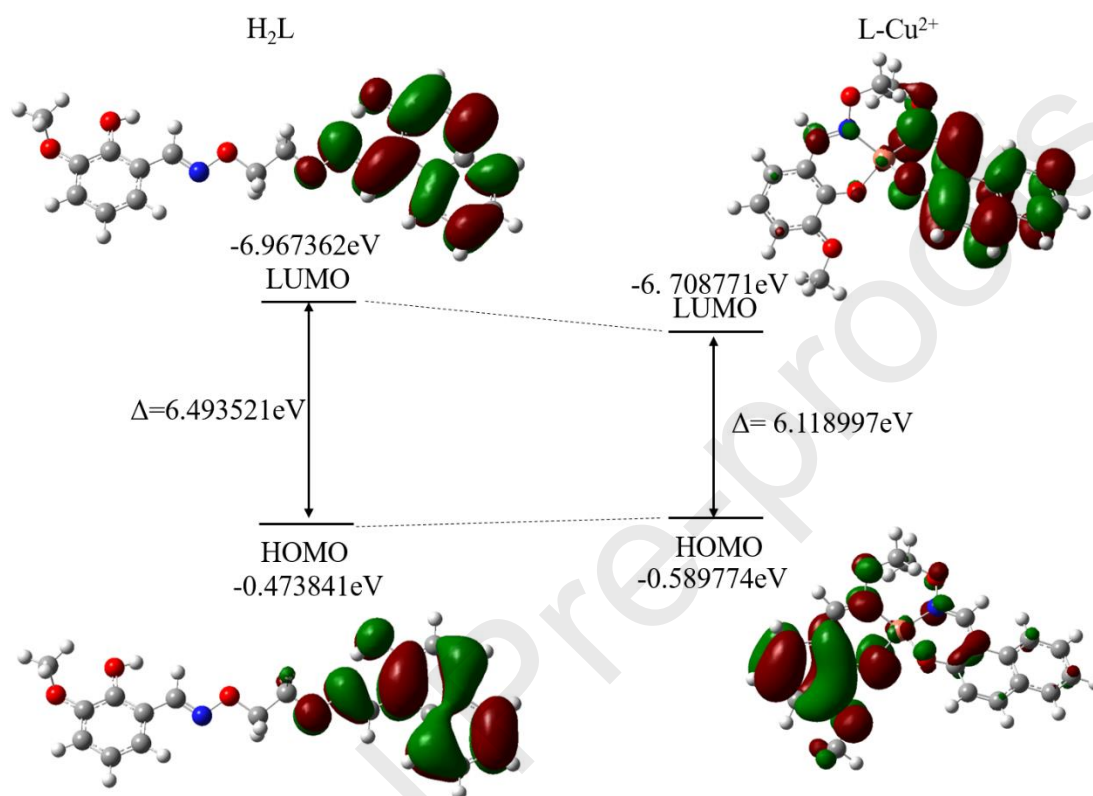


Fig. 7

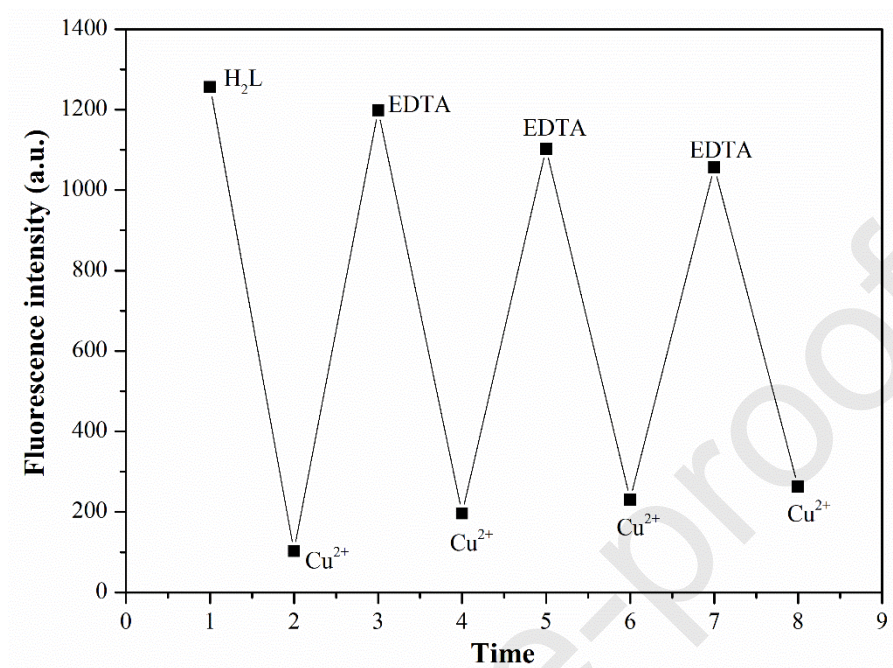
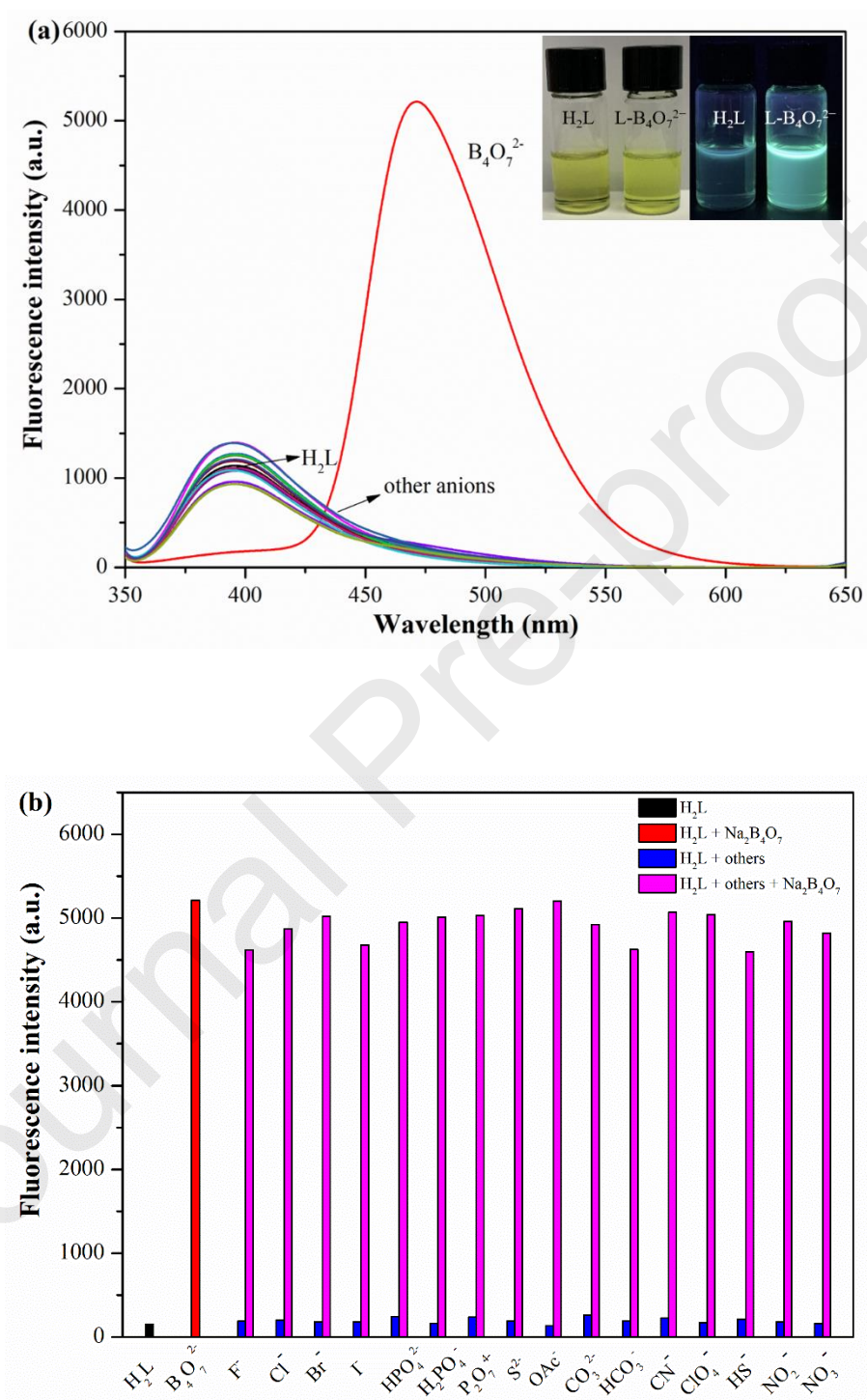


Fig. 8



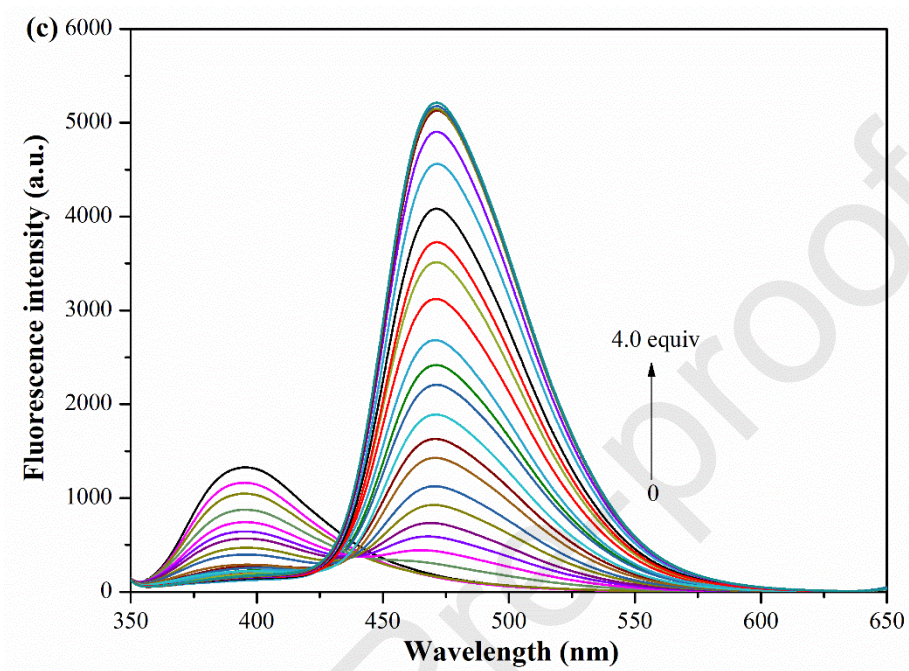
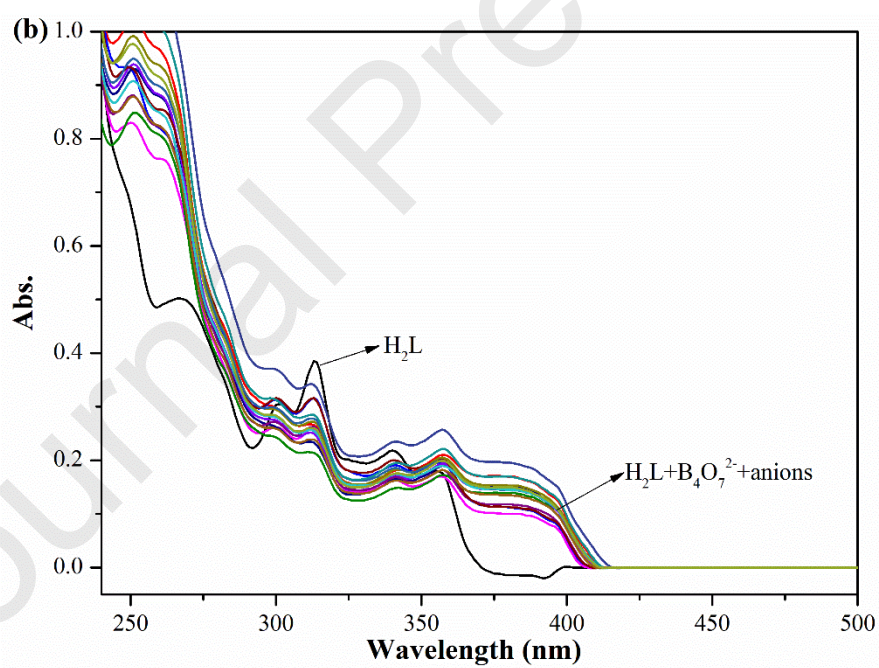
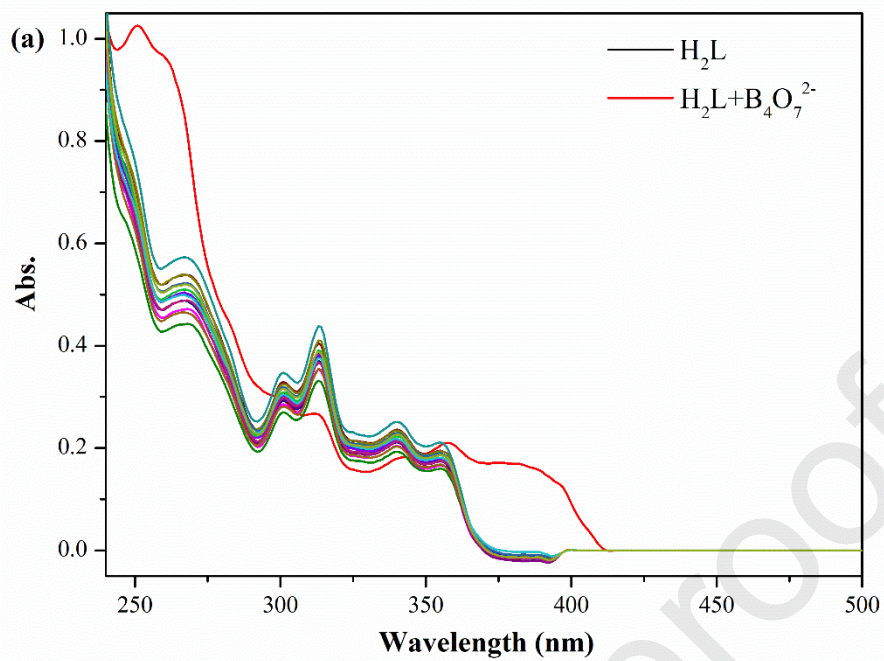


Fig. 9



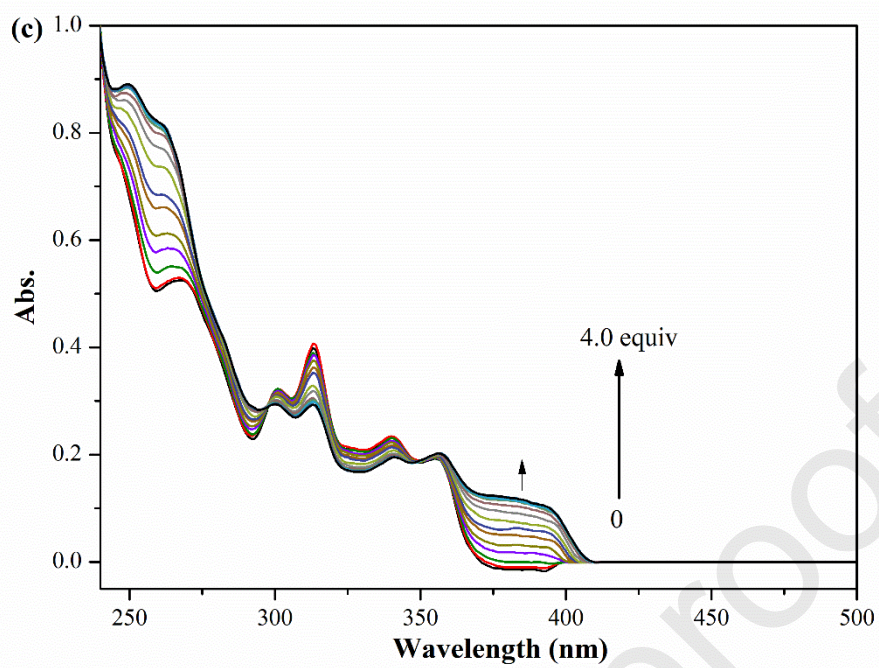


Fig. 10

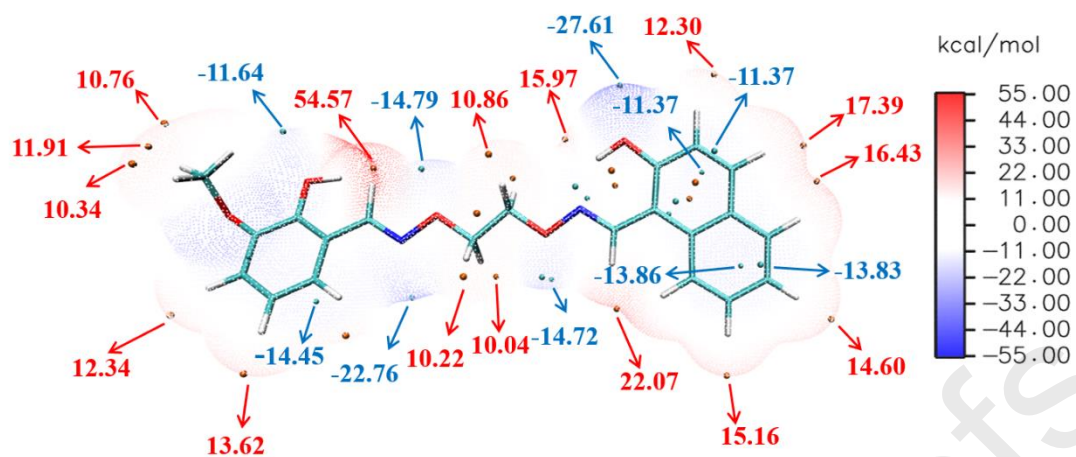


Fig. 11

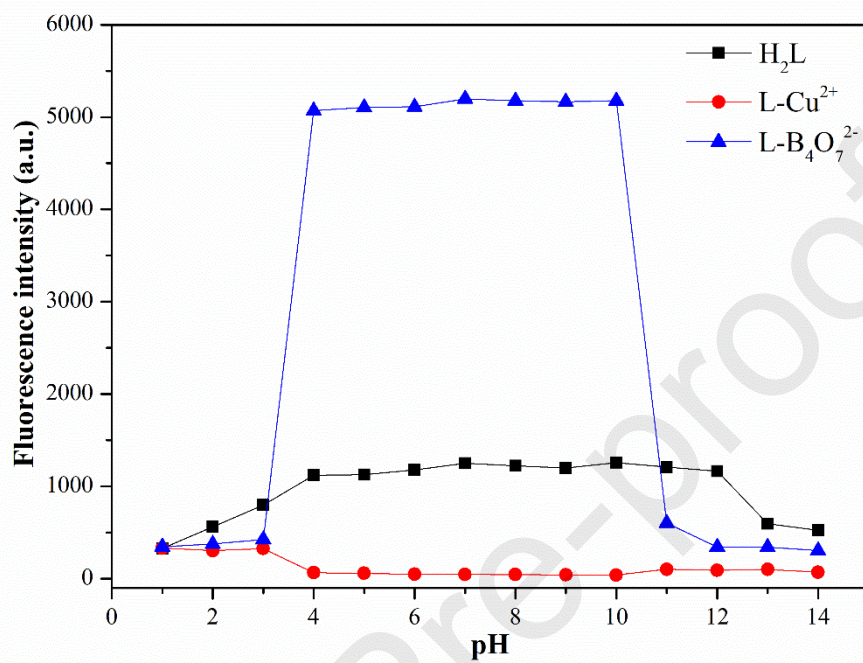


Fig. 12

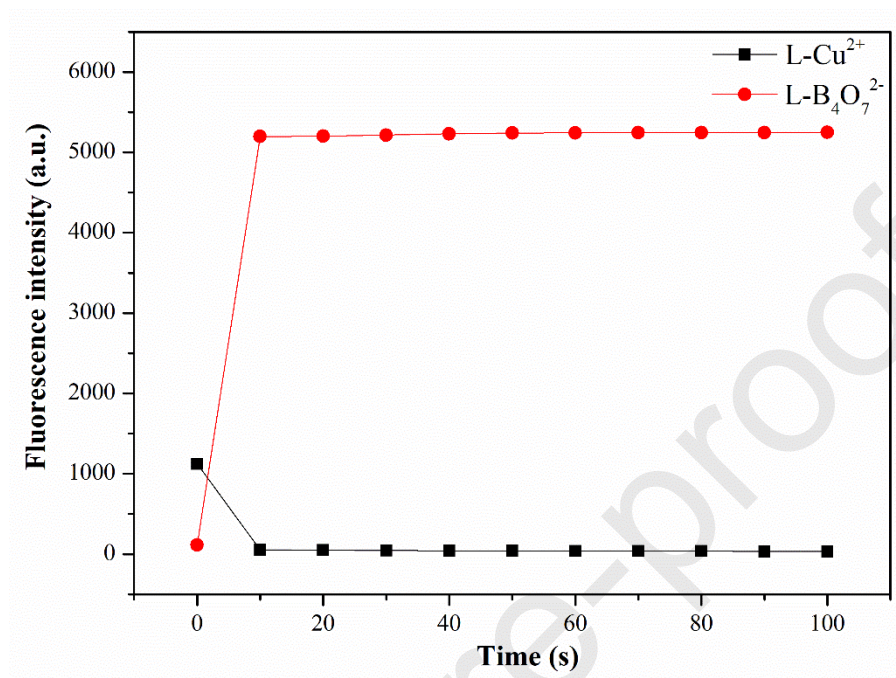


Fig. 13

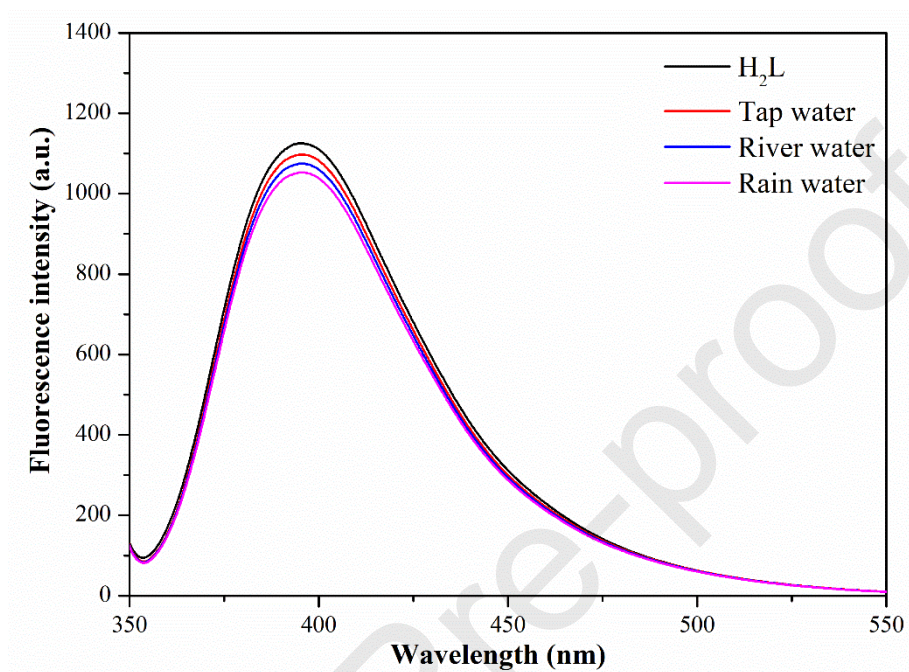


Fig. 14

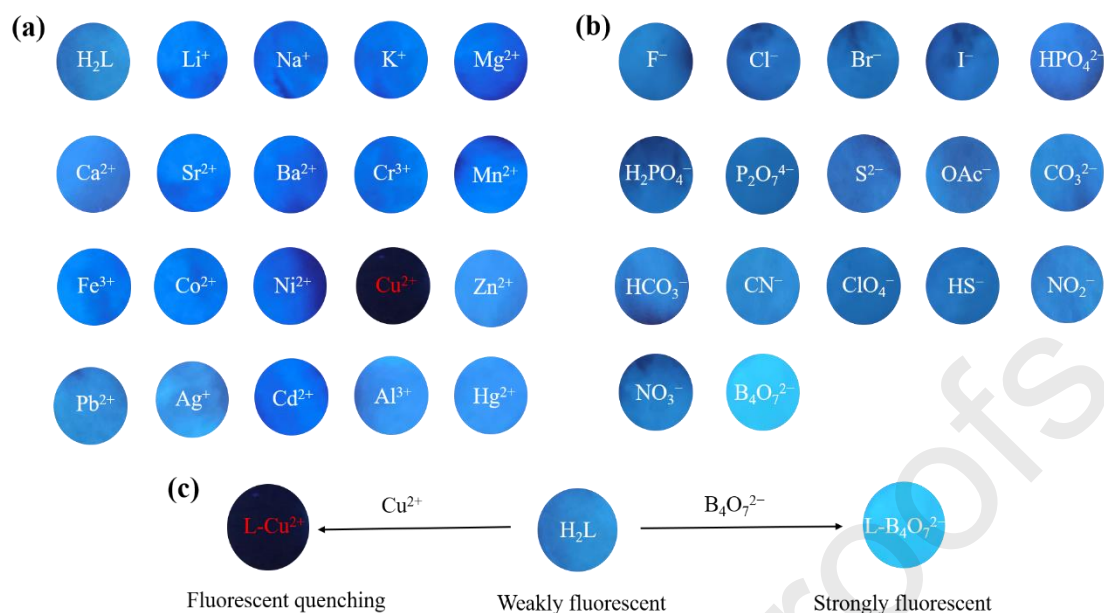


Fig. 15

Research Highlights

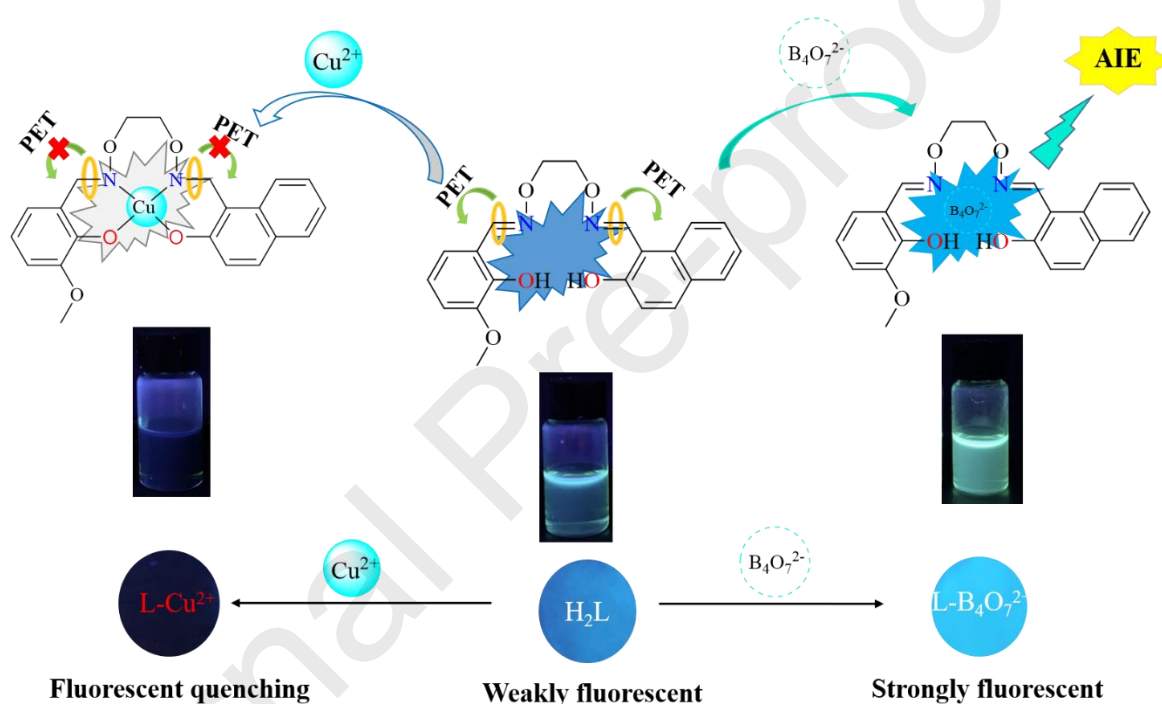
1. The unsymmetric salamo-based chemical sensor **H₂L** was synthesized and characterized structurally.
2. The chemical sensor **H₂L** is fast and sensitive to the recognition of Cu^{2+} and $\text{B}_4\text{O}_7^{2-}$.
3. The chemical sensor **H₂L** has a wide pH range and has an "off-on-off" reversible behavior.
4. Quickly and qualitatively detect Cu^{2+} and $\text{B}_4\text{O}_7^{2-}$ using test strip experiment.

Graphical Abstract

A new type of unsymmetric salamo-based colorimetric and fluorescent chemical sensor **H₂L** was synthesized and characterized. The chemical sensor **H₂L** has an efficient dual channel for Cu^{2+} and $\text{B}_4\text{O}_7^{2-}$ under the solvent conditions of DMF: $\text{H}_2\text{O} = 9: 1$ identify the effect. The chemical sensor **H₂L** can combine with Cu^{2+} to form

a 1: 1 complex, which in turn leads to quenching of fluorescence. Meanwhile, the chemical sensor H_2L has an electron donor capability, due to the introduction of $\text{B}_4\text{O}_7^{2-}$, the density of the electron cloud around the N and O atoms was changed, prompting the fluorophore of the chemical sensor H_2L to produce stronger fluorescence. In addition, the chemical sensor H_2L was also used to detect the Cu^{2+} content in different water samples in life.

Probe for the detection of Cu^{2+} and $\text{B}_4\text{O}_7^{2-}$:



Biographies

Xin Xu is currently pursuing her master's degree in the School of Chemical and Biological Engineering at Lanzhou Jiaotong University, China. She obtained her bachelor's degree in the School of Chemistry and Chemical Engineering of Jining University, China, in 2018.

Ruo-Nan Bian is currently pursuing her master's degree in the School of Chemical and Biological Engineering at Lanzhou Jiaotong University, China. She obtained a bachelor's degree from the College of Chemical Engineering, Lanzhou Jiaotong University, China in 2018.

Shuang-Zhu Guo is currently pursuing her master's degree in the School of

Chemical and Biological Engineering at Lanzhou Jiaotong University, China. He received a bachelor's degree from the College of Chemical Engineering, Harbin Normal University, China in 2018.

Wen-Kui Dong received his PhD degree in 1998 from Lanzhou University, China. He is a professor in the School of Chemical and Biological Engineering at Lanzhou Jiaotong University. His current research interests are focusing on the chemistry of functional supramolecular complexes, materials and new products, as well as processes and applications of environmental chemical engineering.

Yu-Jie Ding received her PhD degree in 2013 from Nanjing University, China; She is an associate professor in College of Biochemical Engineering at Anhui Polytechnic University, her current research interesting is the synthesis and application of upconversion luminescence nanomaterials.

No conflict of interest exists in the submission of this manuscript, and manuscript is approved by all authors for publication. I would like to declare on behalf of my co-authors that the work described was original research that has not been published previously, and not under consideration for publication elsewhere, in whole or in part. All the authors listed have approved the manuscript that is enclosed. In addition, we solemnly declare that the article is original and unpublished and is not being considered for publication elsewhere.